9. Ram Z, Culver WK, Walbridge S, et al. In situ retroviral-mediated gene transfer for the treatment of brain tumors in rats. *Cancer Res* 1993;53:83–88.
10. Keller PM, Fyfe JA, Beauchamp L, et al. Enzymatic phosphorylation of acyclic nucleoside analogs and correlations with antiherpetic activities. *Biochem Pharmacol* 1981;30:3071–3077.
11. Miller AD, Rosman GJ. Improved retroviral vectors for gene transfer and expression. *Bio Techniques* 1989;7:980–990.
12. Zimmerman TP, Mahony WB, Prus KL. 3'-azido-3'deoxythymidine. An unusual nucleoside analogue that permeates the membrane of human erythrocytes and lymphocytes by nonfacilitated diffusion. *J Biol Chem* 1987;262:5748–5754.
13. Sachs L. *Angewandte Statistik*. Berlin. Springer; 1984:329–333.
14. Haberkorn U, Oberdorfer F, Klenner T, et al. Metabolic and transcriptional changes in osteosarcoma cells treated with chemotherapeutic drugs. *Nucl Med Biol* 1994;21:835–845.
15. Higashi K, Clavo AC, Wahl RL. In vitro assessment of 2-fluoro-2-deoxy-D-glucose, L-methionine and thymidine as agents to monitor the early response of a human adenocarcinoma cell line to radiotherapy. *J Nucl Med* 1993;34:773–779.
16. Shields AF, Coonrod DV, Quackenbush RC, Crowley JJ. Cellular sources of thymidine nucleotides: studies for PET. *J Nucl Med* 1987;28:1435–1440.
17. Shields AF, Lim K, Grierson J, Link J, Krohn KA. Utilization of labeled thymidine in DNA synthesis: studies for PET. *J Nucl Med* 1990;1990:31:337–342.
18. Balzarini J, Bohman C, Walker RT, DeClerqu E. Comparative cytostatic activity of different antiherpetic drugs against herpes simplex virus thymidine kinase gene-transfected tumor cells. *Mol Pharmacol* 1994;45:1253–1258.
19. Wohlrab F, Jamieson AT, Hay J, Mengel R, Guschlbauer W. The effect of 2'-fluoro-2'-deoxycytidine on herpes virus growth. *Biochim Biophys Acta* 1985;824: 233–242.
20. Monclus M, Luxen A, Van Naemen J, et al. Development of PET radiopharmaceuticals for gene therapy: synthesis of 9-((1-(^{18}F)fluoro-3-hydroxy-2-propoxy)methyl) guanine. *J Label Comp Radiopharm* 1995;37:193–195.
21. Tjuvajev JG, Stockhammer G, Desai R, et al. Imaging the expression of transfected genes in vivo. *Cancer Res* 1995;55:6126–6132.
22. Bi WL, Parysk LM, Warnick R, Stambrook PJ. In vitro evidence that metabolic cooperation is responsible for the bystander effect observed with HSV-tk retroviral gene therapy. *Hum Gene Ther* 1993;4:725–731.
23. Freeman SM, Abbond CN, Whartenby KA, et al. The "bystander effect": tumor regression when a fraction of tumor mass is genetically modified. *Cancer Res* 1993;53:5274–5283.
24. Chen CY, Chang YN, Ryan P, Linscott M, McGarrity GJ, Chiang YL. Effect of herpes simplex virus thymidine kinase expression levels on ganciclovir-mediated cytotoxicity and the "bystander effect". *Hum Gene Ther* 1995;6:1467–1476.
25. Plagemann PGW, Richey DP. Transport of nucleosides, nucleic acid bases, choline and glucose by animal cells in culture. *Biochem Biophys Acta* 1974;344:263–305.
26. Belt JA, Marina NM, Phelps DA, Crawford CR. Nucleoside transport in normal and neoplastic cells. *Advan Enzyme Regul* 1993;33:235–252.
27. Huang QQ, Yao SYM, Ritzel MWL, Paterson ARP, Cass CE, Young JD. Cloning and functional expression of a complementary DNA encoding a mammalian nucleoside transport protein. *J Biol Chem* 1994;269:17757–17760.
28. Mahony WB, Domin BA, McConnel RT, Zimmerman TP. Acyclovir transport into human erythrocytes. *J Biol Chem* 1988;263:9285–9291.
29. Gati WP, Misra HK, Knaus EE, Wiebe LI. Structural modifications at the 2' and 3' positions of some pyrimidine nucleosides as determinants of their interaction with the mouse erythrocyte nucleoside transporter. *Biochem Pharmacol* 1984;33:3325–3331.
30. Mahony WB, Domin BA, Zimmerman TP. Ganciclovir permeation of the human erythrocyte membrane. *Biochem Pharmacol* 1991;41:263–271.
31. Domin BA, Mahony WB, Zimmerman TP. Membrane permeation mechanisms of 2',3'-dideoxynucleosides. *Biochem Pharmacol* 1993;46:725–729.
32. Haberkorn U, Oberdorfer F, Gebert J, et al. Monitoring of gene therapy with cytosine deaminase: in vitro studies using ^{3}H-5-fluorocytosine. *J Nucl Med* 1996;37:87–94.

Technetium-99m Labeling and Biodistribution of Anti-TAC Disulfide-Stabilized Fv Fragment

Tae M. Yoo, Hye K. Chang, Chang W. Choi, Keith O. Webber, Nhat Le, In S. Kim, William C. Eckelman, Ira Pastan, Jorge A. Carrasquillo and Chang H. Paik

Department of Nuclear Medicine and Positron Emission Tomography Department, Warren G. Magnuson Clinical Center and Laboratory of Molecular Biology, Division of Cancer Biology, Diagnosis and Centers, National Cancer Institute, National Institutes of Health, Bethesda, Bethesda, Maryland

We used a preformed ^{99m}Tc chelate approach to label a genetically engineered disulfide-bonded Fv fragment of anti-Tac monoclonal antibody (dsFv). The biodistribution of this ^{99m}Tc-labeled dsFv was evaluated in athymic mice with IL-2α-receptor-positive ATAC4 tumor xenografts. **Methods:** Benzoylmercaptoacetyl-triglycine (Bz-MAG3) was first labeled with ^{99m}Tc, and the carboxy group of ^{99m}Tc-MAG3 was then activated to the corresponding tetrafluorophenyl ester. This activated ester was purified with a Sep-Pak C_{18} column and conjugated to dsFv. The resulting ^{99m}Tc-MAG3-dsFv was purified with PD-10 size-exclusion chromatography. The immunoreactivity of ^{99m}Tc-MAG3-dsFv was 76% ± 9%. When incubated in serum at 37°C for 24 hr, there was no appreciable dissociation of ^{99m}Tc. The mice were co-injected with ^{125}I-dsFv labeled by the Iodo-Gen method as a control. The mice were killed at 15 to 720 min for analysis of biodistribution and radiocatabolites. **Results:** The tumor uptake of ^{99m}Tc-MAG3-dsFv was similar to that of ^{125}I-dsFv. The tumor uptake of ^{99m}Tc-MAG3-dsFv was rapid with a tumor-to-blood or tumor-to-organ ratio higher than 1 for all organs except the kidneys. The peak tumor value of 5.1% injected dose per gram was obtained at 45 min, and the tumor-to-organ ratios increased steadily over time; a ratio of 15, 11, 7, 95 and 0.10 resulted at 6 hr for blood, liver, stomach, muscle and kidney. The radioactivity was primarily excreted through kidneys. **Conclusion:** The rapid achievement of high tumor-to-blood and -tissue ratios makes ^{99m}Tc-MAG3-dsFv a promising agent for scintigraphic detection of various hematological malignancies that express IL-2α receptors.

Received Dec. 12, 1995; revision accepted Apr. 5, 1996.

For correspondence or reprints contact: Chang H. Paik, PhD, Department of Nuclear Medicine, Bldg. 21, Rm. 136, Bethesda, MD 20892-1180.

Key Words: technetium-99m; Fv fragment; monoclonal antibody; radioimmunodetection; athymic mice

J Nucl Med 1997; 38:294-300

Anti-Tac dsFv is a genetically engineered antibody fragment that consists of portions of the heavy- and light-chain domains linked by an interchain disulfide bridge and binds to the p55 subunit of the IL-2 receptor (*1,2*). This dsFv is different from single-chain Fv (scFv) in that the heavy- and light-chain domains of scFv are linked by a covalent peptide bond (*3–5*). Because of their small size (~25 kDa), these fragments penetrate tumors much faster (*6–8*) and show more uniform distribution (*9,10*) than intact IgG. In addition, it is expected that the fragments are less immunogenic than IgG, thereby minimizing the development of human antimouse immune response (HAMA) (*11,12*). We have previously reported the biodistribution of anti-Tac dsFv radiolabeled with ^{125}I and ^{18}F in athymic mice bearing antigen-positive tumor xenografts (*13*). The blood clearance, whole-body clearance and tumor targeting occurred quickly, suggesting that ^{99m}Tc-labeled dsFv could be used effectively.

Technetium-99m is the ideal isotope for imaging applications. Both direct and indirect methods for ^{99m}Tc labeling of monoclonal antibody have been reported (*14–20*). Direct labeling approaches require reduction of the disulfide bridge to generate sulfhydryl groups for the formation of a stable complex with ^{99m}Tc unless a sulfhydryl-containing amino acid,

such as cysteine is incorporated into Fv through recombinant DNA technology, as shown by George et al. (*21*). Because the disulfide bond is necessary for optimal function of dsFv (*1*), we did not pursue this approach. In this study, we conjugated anti-Tac dsFv to a prelabeled bifunctional chelating agent, ^{99m}Tc-mercaptoacetyltriglycine (^{99m}Tc-MAG3) (*22*), and compared its biodistribution and catabolite formation to that of ^{125}I-labeled dsFv in athymic mice xenografted with the IL-2α-receptor-positive ATAC4 tumor cells.

MATERIALS AND METHODS

Radiolabeling

The production of anti-Tac dsFv has been described (*1*). Anti-Tac dsFv used for this study recognizes the alpha subunit of the IL-2 receptor (*2*), and was more than 98% pure, as determined by a UV monitor on size-exclusion HPLC. Benzoyl-MAG3 (Bz-MAG3) was synthesized according to the method of Fritzberg et al. (*22*) and radiolabeled with ^{99m}Tc using the method of Visser et al. (*23*). Briefly, 150 μl of 1.0 *M* sodium carbonate (pH 11.7), 25 μl of Bz-MAG3 (1 mg/ml in 9:1 acetonitrile:water), 200 μl of [^{99m}Tc] pertechnetate (up to 370 MBq) and 100 μl of stannous chloride monohydrate (1 mg/ml in 0.002 N HCl) were added in a 5-ml glass vial. The vial was rubber-stoppered, evacuated and vortexed gently. The vial was placed in a boiling water bath for 10 min. The reaction solution was then cooled in an ice-water bath and its pH was adjusted to 5.7–6.3 by the addition of 270 μl of 1.0 N sulfuric acid. To this acidified solution, 200 μl of 2,3,5,6-tetrafluorophenol (100 mg/ml of 9:1 acetonitrile:water) and 50 mg of 1-ethyl-3-(3-dimethylaminopropyl)-carbodiimide (EDC) were added. The esterification reaction was performed at room temperature for 30 min with a gentle shaking. The reaction solution was diluted to 8 ml with distilled water and the product, ^{99m}Tc-labeled 2,3,5,6-tetrafluorophenyl ester of MAG3, was purified by a Sep-Pak C18 column (Waters, Milford, MA) as follows. A Sep-Pak column was preconditioned by eluting with 20 ml of acetonitrile and 20 ml of distilled water. The dilute reaction mixture was loaded into the column. The column was sequentially eluted with 20 ml of distilled water, 30 ml of 20% ethyl alcohol in 0.01 *M* sodium phosphate at pH 6.7, 0.5 ml of ethyl ether and finally with acetonitrile. The eluate with acetonitrile was collected in 1-ml fractions. The major radioactivity was eluted in acetonitrile fractions 2 and 3. These fractions were combined and mixed with 10 μl of 0.1 *M* 4-morpholineethanesulfonic acid (MES), pH 5.6. The organic solvent was then evaporated off with a stream of nitrogen gas to the final volume of 10–20 μl. To this solution, 10 μl of N,N-dimethylformamide, 6 μl of 1 *M* sodium bicarbonate, pH 9.5 and 50 μl of dsFv (1.25 mg/ml of phosphate buffered saline (PBS, pH 7.4) were added. The conjugation reaction was performed on an ice bath for 30 min. The conjugation yield was estimated by instant thin-layer chromatography (ITLC, silica gel-impregnated glass fiber, Gelman Sciences, Ann Arbor, MI) developed with 85% methanol in 0.02 *M* sodium phosphate in saline, pH 6.7, and 5% HSA pretreated paper chromatography developed with saline. The final product, ^{99m}Tc-MAG3-dsFv, was purified with size-exclusion PD-10 column chromatography. The purity of the product (retention time = 12.4 min) was confirmed by size-exclusion HPLC equipped with a TSK G2000SW, as described previously (*13*). The purity of the product was also determined by ITLC and paper chromatography, as described above. In the ITLC system, the labeled dsFv stays at the origin of sample application, but ^{99m}Tc-MAG3 and [^{99m}Tc] pertechnetate move with the solvent front. In the paper chromatographic system, radiocolloids stay at the origin, but the labeled dsFv, ^{99m}Tc-MAG3 and [^{99m}Tc]pertechnetate move with the solvent front. The radiochromatograms were obtained using a Bioscan System 300 Imaging Scanner detector (Bioscan Inc., Washington, DC). The total time from the start of radiolabeling to the analysis of the purified product was 4 hr.

To identify catabolites from ^{99m}Tc-MAG3-dsFv, standards for N-ϵ-^{99m}Tc-MAG3-lysine and N-ϵ-^{99m}Tc-MAG3-(N-α-acetyl) lysine were synthesized, with a quantitative yield, by reacting 20 μl of the activated ester of ^{99m}Tc-MAG3 described above with 50 μl of N-α-acetyllysine or lysine at 100 mg/ml in 0.1 *M* sodium bicarbonate, pH 9.5. The reaction yield was determined by reversed-phase (RP) TLC (Uniplate, RPS-F, 5 × 20 cm, Analtech, Inc., Newark, DE), developed with 3% acetonitrile in 5 m*M* sodium phosphate, pH 6.7. The products were also analyzed by RP HPLC equipped with a reversed-phase Radial-Pak cartridge (Delta-Pak C18, 8 × 100 mm, Waters, Millipore Corporation, Milford, MA). The cartridge was eluted with either 3% or 7% acetonitrile in 5 m*M* phosphate buffer, pH 6.7 at 1 ml/min.

The dsFv was also radiolabeled with ^{125}I as previously described (*13*) using the Iodo-Gen method (*24*) and used as a control in the biodistribution studies. The purity of ^{125}I-dsFv was confirmed by the analytical methods described for ^{99m}Tc-MAG3-dsFv.

Immunoreactivity Determination

Immunoreactivity was determined by a modification of the method of Lindmo et al. (*25,26*). A constant concentration (2.5 ng/well) of radiolabeled anti-Tac dsFv was incubated with increasing concentrations of ATAC4 cells in 6-well plates, the cell-bound activity was determined, and the immunoreactivity was then calculated as described previously (*13*). ATAC4 cells used for the immunoreactivity determination were derived from A431, a human epidermoid carcinoma cell line originally obtained from G. Todoro (NIH), by transfection with plasmids encoding IL-2α receptor and a neomycin-resistant gene (*27*).

Biodistribution Studies

Female athymic mice (4–5 wk old, 17–23 g) were used. The mice were inoculated subcutaneously with 3 × 10^6 ATAC4 cells in the left flank. When tumors had reached 0.5 to 1.0 cm in diameter approximately 2 wk after inoculation, the mice were co-injected through the tail vein with ^{99m}Tc-MAG3-dsFv (0.19 MBq/1 μg) and ^{125}I-dsFv (0.09 MBq/1 μg). Groups of five mice were euthanized with CO_2 at 15, 45, 90, 360 and 720 min postinjection. Tumors, organs of interest and blood were weighed and counted in a gamma counter as described previously. These samples and standards were initially counted in the gamma counter using an energy setting of 100–200 keV for ^{99m}Tc. After ^{99m}Tc had decayed, the samples and standards were then recounted using a 15–80 keV setting for ^{125}I photopeak. Counts (cpm) were corrected for decay. The percent injected dose per gram of tissue or blood was calculated and normalized to a 20-g mouse. Tissue-to-blood and tumor-to-tissue ratios were also calculated.

In separate experiments, groups of two nontumor-bearing athymic mice were co-injected with ^{99m}Tc-MAG3-dsFv and ^{125}I-dsFv to evaluate the early-phase blood clearance. Approximately 1 min after injection, serial blood samples were collected through tail vein puncture using a 10-μl calibrated pipette. The blood samples were counted in a gamma counter. The first phase blood clearance half-life was determined by fitting the early clearance up to 10 min with 5 to 6 time points to a single exponential (Sigma plot, Jandel Scientific, CA). Since the beta phase was found to be insignificant, it was not subtracted from the first clearance phase to obtain the alpha phase.

Analysis of Catabolites

The serum and urine samples from groups of two mice were collected at 15, 45 and 90 min and stored in an ice bath until analyzed. Most of these samples were analyzed by three chromato-

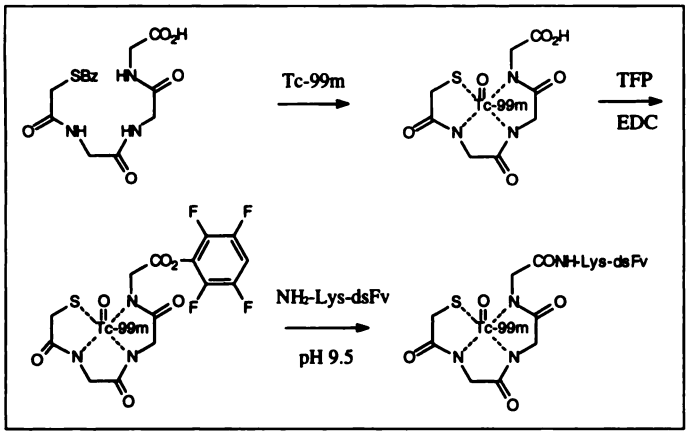

FIGURE 1. Preparation of ^{99m}Tc-MAG3-dsFv.

graphic systems: size exclusion HPLC, RP HPLC and RP TLC. The serum and urine samples were centrifuged for 10 min at 3000 rpm before the analyses. In addition, the serum samples used for RP HPLC were treated dropwise with an equal volume of acetonitrile to precipitate serum proteins and then centrifuged for 10 min at 3000 rpm. The supernatant was pipetted out and the organic solvent in the supernatant was evaporated with a stream of nitrogen gas for 30 min. The serum and urine samples were chromatographed along with iodotyrosine as an internal standard to account for run-to-run variation of sample mobility. To identify radiocatabolites by these chromatographic systems, 3-iodotyrosine, 3-iodo-(N-α-acetyl)tyrosine, [^{125}I]sodium iodide, ^{99m}Tc-MAG3, N-α-acetyllysine adduct and lysine adduct of ^{99m}Tc-MAG3 were used as standards.

Size-exclusion HPLC equipped with a TSK G2000SW column was used to separate radioproteins and radiocatabolites by molecular weight. Molecular weight standards ranging from vitamin B12 (1350 D) to thyroglobulin (670 kD) were used to estimate the molecular weight of the radioproducts. RP HPLC equipped with a reversed-phase Radial-Pak cartridge was used to separate radioactive products by polarity. The cartridge was eluted with either 3% or 7% acetonitrile in 5 m*M* phosphate buffer, pH 6.7 at 1 ml/min. The RP HPLC with 7% acetonitrile showed retention times of 5.4, 5.9 and 10.9 min for [^{99m}Tc]pertechnetate, ^{99m}Tc-MAG3 and N-ϵ-^{99m}Tc-MAG3-(N-α-acetyl)lysine, respectively. Whereas the retention times with 3% acetonitrile were 5.0, 7.8, 32.8 and 35.2 min, respectively, for [^{99m}Tc]pertechnetate, ^{99m}Tc-MAG3, N-ϵ-^{99m}Tc-MAG3-lysine and N-ϵ-^{99m}Tc-MAG3-(N-α-acetyl)lysine. With 7% acetonitrile, the retention times for [^{125}I]iodide, 3-iodotyrosine and 3-iodo-(N-α-acetyl)tyrosine were 4.9, 9.0 and 16 min, respectively. We also used RP TLC (3% acetonitrile in 5 m*M* phosphate buffer, pH 6.7). The Rf values for [^{99m}Tc]pertechnetate, ^{99m}Tc-MAG3 and N-ϵ-^{99m}Tc-MAG3-(N-α-acetyl)lysine were 1.0, 0.78 and 0.36 on this RP TLC. The corresponding Rf values for [^{125}I]sodium iodide, 3-iodotyrosine and 3-iodo-(N-α-acetyl)tyrosine were 1.0, 0.46 and 0.39, respectively.

RESULTS

Radiolabeling, Stability and Immunoreactivity

The preformed chelate approach involved ^{99m}Tc labeling of Bz-MAG3 as the first step reaction (Fig. 1). This step produced ^{99m}Tc-MAG3 in a quantitative yield. The carboxy group of ^{99m}Tc-MAG3 was activated to the corresponding tetrafluorophenyl ester in a 72% yield, as estimated from the percentage of the total ^{99m}Tc activity eluted with acetonitrile in three 1-ml fractions. The conjugation of this activated ester to dsFv was obtained in an average overall recovery yield of 23.9% ± 7.8% (n = 6), as estimated from the radioactivity bound to dsFv

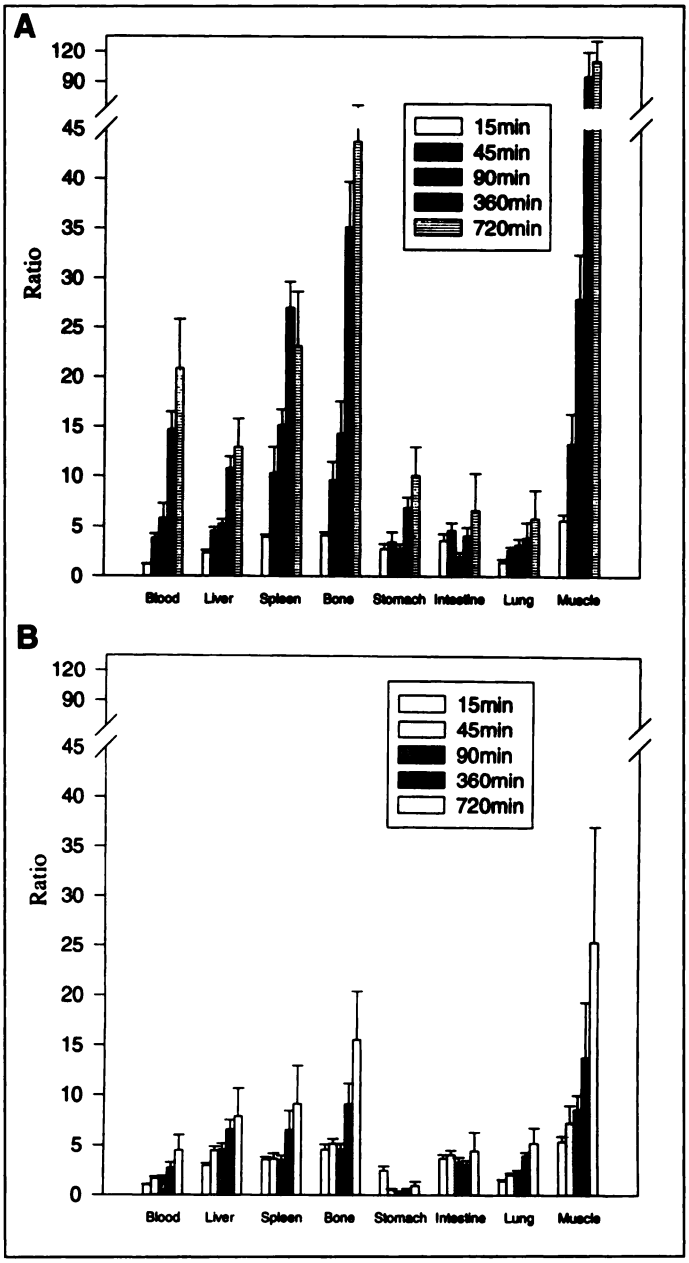

FIGURE 2. Tumor-to-tissue ratio of ^{99m}Tc-MAG3-anti-TAC dsFv (A) and ^{125}I-anti-TAC dsFv (B) in athymic mice bearing IL-2α-receptor-positive (ATAC4) tumor xenografts. The ratio was obtained by dividing the percent injected dose per gram in tumor by that in each tissue at each time point. The ratios with s.d. (bars) were plotted.

purified by PD-10 chromatography. This labeling approach produced ^{99m}Tc-MAG3-dsFv at a specific activity ranging from 5.2 to 30.0 μCi/μg without affecting the immunoreactivity. The immunoreactivity was 76% ± 9% (n = 5), similar to that of ^{125}I-dsFv (79% ± 14%, n = 5). Technetium-99-MAG3-dsFv and ^{125}I-dsFv were stable when incubated with serum in vitro at 37°C with negligible breakdown during 24 hr of observation.

Biodistribution

Both ^{99m}Tc-MAG3-dsFv and ^{125}I-dsFv localized rapidly in the tumor with peak values of 5.05 and 6.51% ID/g, respectively, at 45 min (Table 1) ($p < 0.001$). The concentration of the ^{99m}Tc label (1.93% ID/g) was higher than that of the ^{125}I label (1.15% ID/g) at 12 hr ($p < 0.002$), indicating that the ^{99m}Tc label was retained in the tumor longer. Both tracers cleared more slowly from the tumor than from the blood or most other organs. This resulted in increased tumor-to-nontumor ratios for

TABLE 1
Biodistribution of Technetium-99m- and Iodine-125-Labeled Anti-Tac (dsFv) in Tumor-Bearing Athymic Mice*

Tissue	15 min		45 min	
	^{99m}Tc	^{125}I	^{99m}Tc	^{125}I
Blood	3.76 ± 0.64	4.64 ± 0.99	1.33 ± 0.17	4.03 ± 0.21
Liver	1.87 ± 0.20	1.57 ± 0.25	1.10 ± 0.07	1.47 ± 0.18
Spleen	1.12 ± 0.24	1.33 ± 0.32	0.51 ± 0.15	1.85 ± 0.26
Kidney	268.86 ± 17.17	287.34 ± 13.98	238.83 ± 30.12	189.73 ± 23.74
Bone	1.06 ± 0.17	1.01 ± 0.09	0.53 ± 0.09	1.26 ± 0.16
Stomach	1.58 ± 0.05	1.86 ± 0.37	1.52 ± 0.27	12.25 ± 1.47
Intestine	1.19 ± 0.17	1.25 ± 0.21	1.09 ± 0.11	1.64 ± 0.21
Lung	3.06 ± 0.32	3.37 ± 0.60	1.90 ± 0.36	3.30 ± 0.26
Muscle	0.77 ± 0.08	0.84 ± 0.10	0.39 ± 0.07	0.93 ± 0.21
ATAC4	4.42 ± 0.90	4.62 ± 1.02	5.05 ± 0.65	6.51 ± 0.87

*Data are shown as percent injected dose per gram and reported as mean ± s.d. (n = 5).

most tissues (Fig. 2A, 2B). Although the tumor-to-kidney ratio increased over time for both tracers, at 6 hr it was 0.1 for ^{99m}Tc and 0.3 for ^{125}I, because of the high accumulation of both tracers in kidneys. The rapid sequential blood sampling from the tail showed that the ^{99m}Tc-MAG3-dsFv and ^{125}I-dsFv cleared rapidly from blood. The nonlinear regression analysis of the initial blood clearance data up to 10 min displayed a monoexponential clearance curve, fitting well to the experimental data for both ^{99m}Tc-dsFv and ^{125}I-dsFv (coefficient of variation <9% and $R^2 > 0.98$). Although this curve fitting was achieved with a limited number of data points (six), the small coefficient of variation and R^2 value close to 1 indicate a high degree of curve matching. The initial alpha phase half-life obtained by the nonlinear regression analysis was 3.23 min for the ^{99m}Tc label and 3.28 min for the ^{125}I label. At 15 min, the blood concentrations of the ^{99m}Tc and ^{125}I were 3.76% ± 0.64% and 4.64% ± 0.99% ID/g, respectively (Table 1). The beta phase half-life of the ^{125}I label was somewhat slower than the ^{99m}Tc label, resulting in 1.06% ± 0.47% ID/g versus 0.18% ± 0.02% ID/g remaining in the blood at 6 hr ($p < 0.02$), respectively.

The tissue-to-blood ratio for ^{99m}Tc tended to increase over time for most tissues sampled. In particular, ratios greater than 2:1 were reached in the kidneys, stomach, intestines and lungs, whereas the ratios in bone and muscle were less than 1 and showed little change over time. The tissue-to-blood ratios of ^{125}I-dsFv differed significantly from those of the ^{99m}Tc at later time points, although the tissue-to-blood ratio was similar at 15 min for both tracers. With the exception of tumor, kidney and stomach, no tissue reached ratios greater than 1 for the ^{125}I label (Fig. 3A, B).

Technetium-99m-MAG3- and ^{125}I-dsFv showed large accumulations in the kidneys (Table 1), which represented 64.96% ± 1.67% and 69.50% ± 2.75% of the injected dose at 15 min, respectively. Thereafter, the ^{99m}Tc label cleared more slowly ($t_{1/2}$ = 77.4 min) than the ^{125}I label ($t_{1/2}$ = 42.2 min). Although the ^{125}I label cleared from kidney faster than the ^{99m}Tc label, higher retention of the ^{125}I label in stomach, blood and perhaps in thyroid made the whole-body retention time of the ^{125}I label longer than that of the ^{99m}Tc label ($t_{1/2}$ of 85.1 min versus 140.7 min, respectively) (Fig. 4).

Analysis of Catabolites

The size-exclusion HPLC analysis separated the parent compound from radiocatabolites. This HPLC analysis of serum samples showed two radioprotein peaks containing ^{99m}Tc and ^{125}I, with retention times of 9.6 and 12.4 min. The 9.6- and 12.4-min peaks correspond to the molecular weights of 160 kD and 25 kD, respectively, as estimated by extrapolation of the retention times to the molecular standard curve. Two small ^{99m}Tc catabolite peaks were seen with retention times of 15.6 and 17.0 min. The molecular weights of the 15.6- and 17.0-min peaks could not be accurately determined because the retention times of these small molecules were also affected by the polarity of molecules. However, the retention time of 15.6 min was identical to that for the standard N-ε-^{99m}Tc-MAG3-(N-α-acetyl)lysine, and the retention time of 17 min was identical to the retention time for both ^{99m}Tc-MAG3 and [^{99m}Tc]pertechnetate.

The relative intensity of the radiolabeled dsFv peak decreased while the relative intensities of the higher molecular weight peak and the radiocatabolite peaks increased over time for serum samples. At 15 min, the ^{99m}Tc-dsFv peak accounted for approximately 75% of the total peak intensity and decreased to 29% at 90 min. During this time, the fraction of the ^{99m}Tc high molecular weight substance (160 kD) increased from 17% to 46%, whereas the fraction of the total ^{99m}Tc catabolites remained unchanged, with 20% at 15 min and 22% at 90 min. For urine samples, the fraction of ^{99m}Tc-dsFv was 51% at 15 min, but by 45 min > 95% of the total urine ^{99m}Tc activity was found with the small catabolites. In comparison, the disappearance of ^{125}I-dsFv from serum was much faster, with 48% of the total serum activity present as ^{125}I-dsFv at 15 min and then decreasing to 9% at 90 min. During this time period, a small ^{125}I catabolite increased from 21% to 67%, whereas the ^{125}I high molecular weight substance remained at 31% to 25%. The analysis of urine samples showed 59% ^{125}I-dsFv at 15 min but only 2% ^{125}I-dsFv at 45 min with all remaining activity associated with one small ^{125}I catabolite.

To identify the catabolites, the urine samples collected at 15, 45 and 90 min were further analyzed by RP TLC and RP HPLC. These analyses showed two minor ^{99m}Tc catabolites with mobilities identical to those of ^{99m}Tc-MAG3 and [^{99m}Tc]pertechnetate. The mobility of the major catabolite was much slower than those of the minor catabolites, especially on RP HPLC eluted with 3% acetonitrile. Its retention time of 32.2 min on RP HPLC was similar to that of N-ε-^{99m}Tc-MAG3-lysine (32.8 min) rather than that of N-ε-^{99m}Tc-MAG3-(N-α-acetyl)lysine (35.2 min). However, we could not disprove ^{99m}Tc-MAG3-(N-α-acetyl)lysine as the major catabolite because the major catabolite did not separate from N-ε-^{99m}Tc-MAG3-(N-α-acetyl)lysine when the urine sample was co-injected with N-ε-^{99m}Tc-MAG3-(N-α-acetyl)lysine on this RP HPLC. We think that the identification of the major catabolite

TABLE 1
Continued

90 min		360 min		720 min	
^{99m}Tc	^{125}I	^{99m}Tc	^{125}I	^{99m}Tc	^{125}I
0.77 ± 0.10	3.75 ± 0.41	0.18 ± 0.02	1.06 ± 0.47	0.09 ± 0.01	0.27 ± 0.08
0.83 ± 0.10	1.31 ± 0.20	0.25 ± 0.01	0.42 ± 0.17	0.15 ± 0.00	0.15 ± 0.04
0.29 ± 0.02	1.73 ± 0.17	0.10 ± 0.01	0.42 ± 0.08	0.09 ± 0.02	0.14 ± 0.05
119.22 ± 35.10	74.97 ± 24.71	28.92 ± 7.56	7.95 ± 2.66	13.88 ± 3.40	0.98 ± 0.22
0.31 ± 0.08	1.31 ± 0.23	0.08 ± 0.01	0.27 ± 0.08	0.05 ± 0.03	0.08 ± 0.02
1.61 ± 0.34	20.21 ± 5.92	0.38 ± 0.07	4.91 ± 1.53	0.20 ± 0.04	1.43 ± 0.37
2.35 ± 0.68	1.87 ± 0.38	0.65 ± 0.11	0.80 ± 0.13	0.33 ± 0.09	0.29 ± 0.11
1.38 ± 0.15	2.66 ± 0.29	0.79 ± 0.36	0.61 ± 0.07	0.40 ± 0.18	0.22 ± 0.04
0.16 ± 0.01	0.72 ± 0.21	0.03 ± 0.01	0.19 ± 0.07	0.02 ± 0.00	0.05 ± 0.02
4.37 ± 0.72	5.95 ± 1.17	2.70 ± 0.32	2.64 ± 0.64	1.93 ± 0.43	1.15 ± 0.21

*Data are shown as percent injected dose per gram and reported as mean ± s.d. (n = 5).

requires additional studies using several different analytical methods. In contrast, using the same system, the analysis of urine samples for ^{125}I catabolite showed only one radiocatabolite with the mobility identical to that of [^{125}I] iodide.

DISCUSSION

Radiolabled antibodies offer great potential specificity for tumor imaging. Nevertheless, the low tumor-to-nontumor ratios seen with many radiolabeled IgG antibodies and the delay in optimal imaging time, often 3–5 days after injection, have impeded the success of many radiolabeled antibody preparations. Preclinical studies suggest that these impediments may be overcome by radiolabeled dsFv fragments. We therefore evaluated a ^{99m}Tc-labeled anti-TAC dsFv and compared its biodistribution to that of ^{125}I-labeled dsFv.

The preformed chelate approach ensured the attachment of ^{99m}Tc to dsFv exclusively via the MAG3 moiety and not directly to amino acid residues of dsFv. This approach provided ^{99m}Tc-labeled dsFv with a high immunoreactivity (76%) which was comparable to that of ^{125}I-labeled dsFv using Bolton-Hunter agent (*28*) or that of ^{18}F-labeled dsFv using N-succinimidyl-4-[^{18}F]-(fluoromethyl)benzoate (*29*). These are also specific agents for labeling dsFv at the amino group of amino acid residues such as lysine.

The tumor targeting of both ^{99m}Tc and ^{125}I labeled anti-Tac dsFvs was fast; peak tumor uptake occurred by 45 min. These rapid kinetics are similar to our previous findings (*13*) and to those of other Fv studies (*6,7,21,28,30*). This indicates that the ^{99m}Tc labeling methodology did not alter tumor uptake. The tumor uptake of this ^{125}I was similar (at 90 and 360 min, $p > 0.5$) or greater (at 15 and 45 min, $p < 0.03$) than that of the ^{125}I reported previously (*13*). The cause of this run-to-run variation in tumor uptake is not well understood. However, the tumors used in this study were generally smaller than those used previously and, thus, possibly more viable.

Although the peak tumor uptake occurred early, the tumor-to-blood ratios continued to increase for both the ^{99m}Tc and ^{125}I preparations, reaching a ratio of 21:1 for the ^{99m}Tc and 4:1 for the ^{125}I at 12 hr (Fig. 2A, B). The increasing tumor-to-blood ratios suggest specific uptake and retention of the ^{99m}Tc in ATAC4 tumor. The lower ratio for ^{125}I is likely due to the somewhat faster clearance of ^{125}I from the tumor and the higher blood levels of ^{125}I. In addition to the tumor-to-blood ratios, the tumor-to-tissue ratios generally increased for both preparations (Fig. 2A, B), reaching values greater than 2, by 45 min for all tissues except the kidney. Since these high tumor-to-nontumor ratios are optimal for imaging and are achieved rapidly, they should allow imaging with a short-life radionuclide such as ^{99m}Tc. The tumor-to-blood ratio for this ^{125}I was higher than that of the previous ^{125}I ($p < 0.01$). However, the tissue-to-blood ratios were generally similar to each other for both ^{125}I dsFv studies.

The initial blood clearance of both the ^{99m}Tc and ^{125}I preparations was similar, as shown by the early serial blood-pool sampling performed within the first 15 min postinjection. These clearance kinetics from blood are similar to those reported by us (*13*) and others (*6,7,21,28,30*). The production of catabolites occurs rapidly and was responsible for the higher concentration of ^{125}I in the blood, suggesting that ^{125}I catabolite reenters the circulation.

Accumulation in the kidney was expected for both the ^{99m}Tc and ^{125}I dsFv, since the dsFvs are filtered due to their small size (~25 kD). Previous studies with antibody fragments have shown that glomerular filtration and subsequent catabolism occurred in the kidneys (*31,32*). While both ^{99m}Tc and ^{125}I preparations showed similar kidney accumulation at 15 min (65.9% and 69.5% injected dose, respectively), the ^{99m}Tc was released from the kidney more slowly than the ^{125}I. This differential release is not unique to ^{99m}Tc and has been previously reported with radiometals (*33–35*). The high accumulation of both tracers in the kidney is problematic for imaging of tumors near the kidney. Attempts to block renal accumulation of radiometals with amino acid infusions have been successful in animal models (*36*) and, to a limited extent, in the clinic (*37*); these approaches also appear to work with ^{99m}Tc-MAG3-dsFv (unreported personal observation) and warrant further clinical evaluation.

The fraction of radioactivity circulating as a high molecular weight substance (160 kD) in the blood became more pronounced at the later time points when the labeled dsFv had cleared from the blood. However, the absolute concentration of this high molecular weight substance in blood was similar for both dsFv labels and was less than 1% ID/g at 90 min postinjection. We do not know the identity of this high molecular weight substance, but it is likely a protein substance present in the original dsFv.

As seen in our previous study, ^{125}I-dsFv or its catabolite did not accumulate appreciably in any normal organs except the kidney, stomach and thyroid. The retention is not surprising since kidney is the major route of dsFv excretion. Once ^{125}I antibodies are catabolized to [^{125}I]iodide, these organs are the main target organs accumulating free iodide. In contrast, the ^{99m}Tc dsFv or its catabolites showed predominant accumulation

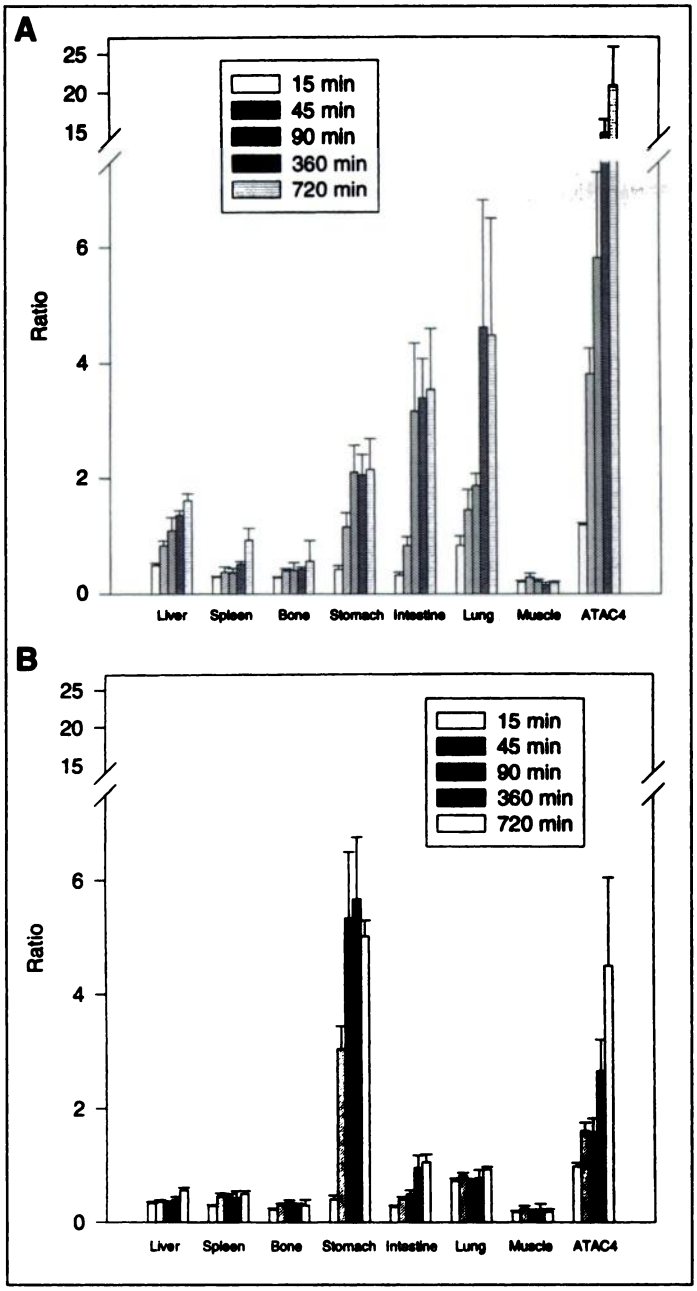

FIGURE 3. Organ-to-blood ratio of ^{99m}Tc-MAG3-anti-TAC dsFv (A) and ^{125}I-anti-TAC dsFv (B) in athymic mice bearing IL-2α-receptor-positive (ATAC4) tumor xenografts. The ratio was obtained by dividing the percent injected dose per gram in each organ by that in the blood at each time point. The ratios with s.d. (bars) were plotted.

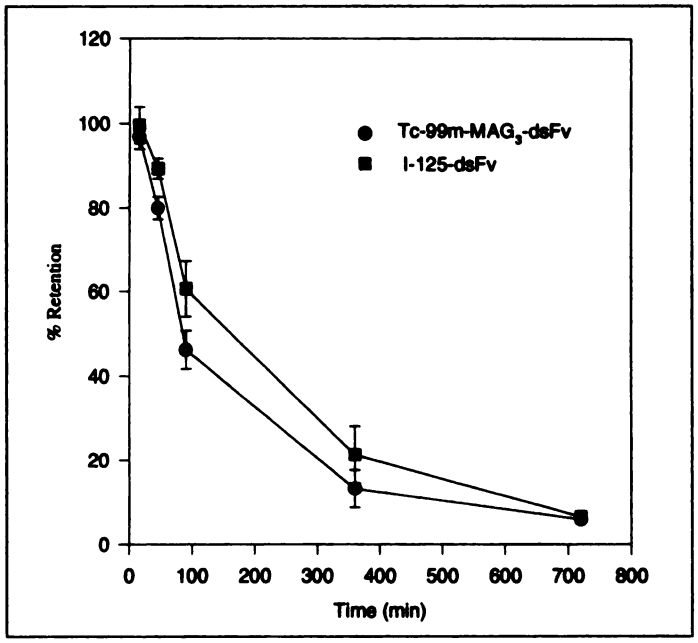

FIGURE 4. Whole-body clearance of radiolabeled anti-TAC dsFv fragments in athymic mice (n = 5) bearing IL-2α-receptor-positive (ATAC4) tumor xenografts. Serial whole-body retention measurements were performed after intravenous co-infusion of ^{99m}Tc-MAG3-dsFv and ^{125}I-dsFv (0.19 MBq/1 μg ^{99m}Tc-MAG3-dsFv and 0.09 MBq/1 μg ^{125}I-dsFv). The radioactivity was measured using a NaI gamma counter. The percent injected dose with s.d. was plotted.

only in the kidney (Table 1). This difference in the pharmacokinetics is likely related to the difference in the formation and excretion of radiocatabolites, since the tissue-to-blood ratios of both radionuclides at 15 min were similar for these organs. As we have shown previously using ^{18}F- and ^{125}I-labeled dsFv, the production of catabolites was rapid. Our study indicates that ^{125}I-labeled dsFv was catabolized rapidly to [^{125}I]iodide perhaps through the formation of N-α-acetyl iodotyrosine and subsequent deiodination by active deiodinases in kidneys, and the iodide diffused out readily into the circulation as shown by the analysis of serum and urine samples (*13,38*). The ^{99m}Tc-MAG3-dsFv was catabolized primarily to an amino acid adduct of ^{99m}Tc-MAG3, with a RP HPLC retention time similar to that of N-ϵ-^{99m}Tc-MAG3-lysine or N-ϵ-^{99m}Tc-MAG3-(N-α-acetyl) lysine, and a minor catabolite with a retention time identical to ^{99m}Tc-MAG3. However, the catabolism of the ^{99m}Tc label appears to take place more slowly than that of the ^{125}I label. These results suggest that the insertion of a readily metabolizable linkage, such as ester, between MAG3 and dsFv might enhance the formation of radiocatabolites and thus increase the renal excretion (*39*).

CONCLUSION

Anti-Tac dsFv was labeled with ^{99m}Tc successfully using a preformed chelate approach without altering the immunoreactivity. The resulting ^{99m}Tc-MAG3-dsFv rapidly localized in ATAC4 tumor, achieving high tumor-to-nontumor ratios. This study suggests that this ^{99m}Tc agent should be considered for tumor imaging. Further studies are needed to improve its pharmacokinetic property in the kidney.

ACKNOWLEDGMENTS

We thank Dr. Virendar K. Sood for providing Benzoyl MAG3 and Mark H. Rotman for editorial assistant.

REFERENCES

1. Webber KO, Reiter Y, Brinkmann U, Kreitman R, Pastan I. Preparation and characterization of a disulfide-stabilized Fv fragment of the anti-Tac antibody: comparison with its single-chain analog. *Mol Immunol* 1995;32:249–258.
2. Uchiyama T, Broder S, Waldmann TAA. A monoclonal antibody (anti-Tac) reactive with activated and functionally mature T-cells. I. Production of anti-Tac monoclonal antibody and distribution of Tac$^+$ cells. *J Immunol* 1981;126:1393–1397.
3. Whitlow M, Bell BA, Feng SL, et al. An improved linker for single-chain Fv with reduced aggregation and enhanced proteolytic stability. *Protein Engineering* 1993;6: 989–995.
4. Pantoliano MW, Bird RE, Johnson LS, et al. Conformational stability, folding and ligand-binding affinity of single-chain Fv immunoglobulin fragments expressed in *Escherichia coli*. *Biochemistry* 1991;30:10117–10125.
5. Huston JS, McCartney J, Tai MS, et al. Medical applications of single-chain antibodies. *Int Rev Immunol* 1993;10(2–3):195–217.
6. Milenic DE, Yokota T, Filpula DR, et al. Construction, binding properties, metabolism and tumor targeting of a single-chain Fv derived from the pancarcinoma monoclonal antibody CC49. *Cancer Res* 1991;51:6363–6371.
7. Adams GP, McCartney JE, Tai MS, et al. Highly specific in vivo tumor targeting by monovalent and divalent forms of 741F8 anti-c-*erb*B-2 single-chain Fv. *Cancer Res* 1993;53:4026–4034.
8. King DJ, Mountain A, Adair JR, et al. Tumor localization of engineered antibody fragments. *Antibod Immunoconj Radiopharm* 1992;5:159–168.
9. Yokota T, Milenic DE, Whitlow M, Schlom J. Rapid tumor penetration of a single-chain Fv and comparison with other immunoglobulin forms. *Cancer Res* 1992;52:3402–3408.

10. Yokota T, Milenic DE, Whitlow M, et al. Microautoradiographic analysis of the normal organ distribution of radioiodinated single-chain Fv and other immunoglobulin forms. *Cancer Res* 1993;53:3776–3783.
11. Reynolds JC, Del Vecchio S, Sakahara H, et al. Antimurine antibody response to mouse monoclonal antibodies: clinical findings and implications. *Nucl Med Biol* 1989;16:121–125.
12. Sakahara H, Reynolds JC, Carrasquillo JA, et al. In vitro complex formation and biodistribution of mouse antitumor monoclonal antibody in cancer patients. *J Nucl Med* 1989;30:1311–1317.
13. Choi CW, Lang L, Lee JT, et al. Biodistribution of ^{18}F- and ^{125}I-labeled anti-Tac disulfide-stabilized Fv fragment in nude mice with IL-2α-receptor-positive tumor xenografts. *Cancer Res* 1995;55:5323–5329.
14. Paik CH, Phan LNB, Hong JJ, et al. The labeling of high affinity sites of antibodies with ^{99m}Tc. *Nucl Med Biol* 1985;12:3–8.
15. Pak KY, Nedelman MA, Tam SH, et al. Labeling and stability of radiolabeled antibody fragments by a direct ^{99m}Tc-labeling method. *Nucl Med Biol* 1992;19:669–677.
16. Rhodes BA, Zamora PO, Nowell KD, Valdez EF. Technetium-99m labeling of murine monoclonal antibody fragments. *J Nucl Med* 1986;27:685–693.
17. Eckelman WC, Paik CH, Steigman J. Three approaches to radiolabeling antibodies with ^{99m}Tc. *Nucl Med Biol* 1989;16:171–176.
18. Thakur ML, DeFulvia JD. Technetium-99m-monoclonal antibodies for immunoscintigraphy. Simplified preparation and evaluation. *J Immunol Methods* 1991;137:217–224.
19. Hnatowich DJ, Mardirossian G, Ruschowski M, et al. Directly and indirectly technetium-99m-labeled antibodies; a comparison of in vitro and animal in vivo properties. *J Nucl Med* 1993;34:109–119.
20. Eckelman WC. Radiolabeling with Tc-99m to study high-capacity and low-capacity biochemical systems. *Eur J Nucl Med* 1995;22:249–263.
21. George ATJ, Jamar F, Tai M, et al. Radiometal labeling of recombinant proteins by a genetically engineered minimal chelation site: Tc-99m coordination by single-chain Fv antibody fusion proteins through a C-terminal cysteinyl peptide. *Proc Natl Acad Sci USA* 1995;92:8358–8362.
22. Fritzberg AR, Kasina S, Eshima D, Johnson DL. Synthesis and biological evaluation of technetium-99m MAG3 as a hippuran replacement. *J Nucl Med* 1986;27:111–116.
23. Visser GWM, Gerretsen M, Herscheid JDM, Snow GB, Dongen G. Labeling of monoclonal antibodies with Rhenium-186 using the MAG3 chelate for radioimmunotherapy of cancer: a technical protocol. *J Nucl Med* 1993;34:1953–1963.
24. Fraker PJ, Speck JC Jr. Protein and cell membrane iodinations with a singly soluble chloramine 1,3,4,6-tetrachloro-3α,6α-diphenylglycouracil. *Biochem Biophy Res Commun* 1978;80:849–857.
25. Lindmo T, Boven E, Cuttitta FJF, Bunn PA Jr. Determination of the immunoreactive fraction of radiolabeled monoclonal antibodies by linear extrapolation to binding at infinite antigen excess. *J Immunol Meth* 1984;72:77–89.
26. Camera L, Kinuya S, Pai LH, et al. Pre-clinical evaluation of ^{111}In-labeled B3 monoclonal antibody: biodistribution and imaging studies in nude mice bearing human epidermoid carcinoma xenografts. *Cancer Res* 1993;53:2834–2839.
27. Kreitman RJ, Bailon P, Chaudhary VK, FitzGerald DJP, Pastan I. Recombinant immunotoxins containing anti-tac(Fv) and derivatives of pseudomonas exotoxin produce complete regression in mice of an interleukin-2 receptor-expressing human carcinoma. *Blood* 1994;83:426–434.
28. Webber KO, Kreitman R, Pastan I. Rapid and specific uptake of anti-Tac disulfide-stabilized Fv by IL-2 receptor-bearing tumors. *Cancer Res* 1995;55:318–323.
29. Lang L, Eckelman WC. One-step synthesis of ^{18}F labeled [^{18}F]-N-succinimidyl 4-(fluoromethyl)benzoate for protein labeling. *Appl Radiat Isot* 1994;45:1155–1163.
30. Colcher D, Bird R, Roselli M, et al. In vivo tumor targeting of a recombinant single-chain antigen-binding protein. *J Natl Cancer Inst* 1990;82:1191–1197.
31. Wochner RD, Strober W, Waldmann TA. The role of the kidney in the catabolism of Bence Jones proteins and immunoglobulin fragments. *J Exper Med* 1967;126:207–221.
32. Arend WP, Silberblatt FJ. Serum disappearance and catabolism of homologous immunoglobulin fragments in rats. *Clin Exper Immunol* 1975;22:502–513.
33. Schott ME, Milenic DE, Yokota T, et al. Differential metabolic patterns of iodinated versus radiometal chelated anticarcinoma single-chain Fv molecules. *Cancer Res* 1992;52:6413–6417.
34. Andrew SM, Perkins AC, Pimm MV, Baldwin RW. A comparison of iodine- and indium-labeled anti-CEA intact antibody, F(ab')$_2$ and F(ab) fragments by imaging tumor xenografts. *Eur J Nucl Med* 1988;13:598–604.
35. Brown BA, Comeau RD, Jones PL, et al. Pharmacokinetics of monoclonal antibody B72.3 and its fragments labeled with either ^{125}I or ^{111}In. *Cancer Res* 1987;47:1149–1154.
36. Pimm MV, Gribben SJ. Prevention of renal tubule re-absorption of radiometal (indium-111) labeled Fab fragment of a monoclonal antibody in mice by systemic administration of lysine. *Eur J Nucl Med* 1994;21:663–665.
37. Hammond PJ, Wade AF, Gwilliam ME, et al. Amino acid infusion blocks renal tubular uptake of an indium-labeled somatostatin analogue. *Br J Cancer* 1993;67:1437–1439.
38. Brown-Grant K. Extrathyroidal iodide concentrating mechanisms. *Physiol Rev* 1961; 41:189–213.
39. Paik CH, Yokohama K, Reynolds JC, et al. Reduction of background activities by introduction of a diester linkage between antibody and a chelate in radioimmunodetection of tumor. *J Nucl Med* 1989;30:1693–1701.